communications medicine

A Nature Portfolio journal

Article

https://doi.org/10.1038/s43856-025-01164-3

Blood and tissue correlates of steroid non-response in checkpoint inhibition-induced immune-related adverse events

Mick J. M. van Eijs[1,2,3], M. Marlot van der Wal[2], Hedi-Britt Klotškova[2], Noël M. M. Dautzenberg[2,3], Mark Schuiveling[1], Rik J. Verheijden[1,4], Fiona D. M. van Schaik[5], Bas Oldenburg[5], Stefan Nierkens[2,3], the UNICIT Consortium*, Karijn P. M. Suijkerbuijk[1,6] & Femke van Wijk[2,6]

Abstract

Background High-dose steroids constitute the cornerstone of first-line treatment for immune-related adverse events (irAEs) associated with immune checkpoint inhibitors, but compromise antitumor immunity. A deeper understanding of irAEs and their response to steroids can improve management.

Methods Using a multi-omics approach, we investigated blood- and tissue-based correlates of steroid response, focusing on gastro-intestinal irAEs, in the largest cohort to date.

Results Here we show clear trends for elevated T_C1/T_C17 $CD8^+$ T cells and Th1/Th17-associated interleukins before steroid initiation, and persistent ($CD8^+$) T cell activation after initiation of steroids in blood of steroid non-responders. Cross-sectional analysis of colitis tissue suggested lower lymphocyte infiltration within 24 h in steroid responders. Peripheral T cell PD-1 receptor occupancy was unrelated to steroid response. Non-responders' colitis tissue was enriched with activated $CD4^+$ memory T cells and a pronounced type 1/17 immune response.

Conclusions These findings highlight rapid steroid effects on circulating cells and irAE-affected tissue and support that an enhanced type 1/type 17 response may be associated with steroid non-response in irAEs. Validation of these findings in larger cohorts is warranted.

Plain language summary

Cancer treatment with immune checkpoint inhibitors can cause side effects, known as immune-related adverse events. Usual first-line treatment consists of corticosteroids, but not all patients with side effects respond to corticosteroids. Moreover, corticosteroids can limit how well checkpoint inhibitor treatment works. This study explored if response to corticosteroids can be predicted and what factors determine response to corticosteroids. To this end, we investigated blood and gut tissue from patients with side effects, mostly affecting the stomach and gut. We found that certain types of immune cells and signaling substances were elevated in blood and tissue from patients with side effects who did not respond to steroids. These findings may help identify patients who require other immunosuppressive drugs than corticosteroids to treat their side effects. This study can also contribute to new treatments for side effects of immune checkpoint inhibitors.

Immune checkpoint inhibition (ICI) has revolutionized the field of oncology, with expanding indications across tumor types and in both early and advanced disease stages[1]. Unfortunately, ICI comes with severe immune-related adverse events (irAEs) in up to 60% of patients treated with combined anti-programmed death-1 (anti-PD-1) plus anti-cytotoxic T-lymphocyte-associated protein-4 (anti-CTLA-4)[1]. Most severe irAEs do not resolve spontaneously without immunosuppressive treatment and can become chronic, or even fatal, if left untreated[1]. Clinical guidelines empirically advise to treat irAEs, depending on Common Terminology Criteria for Adverse Events (CTCAE) severity grade, with moderate-to-high doses of systemic steroids in first line (typically 1 or 2 mg/kg daily prednisone-equivalence for some grade 2 and most grade 3-4 irAEs)[2–4]. If symptoms do not improve within 3–5 days, escalation to higher-dosed

[1]Department of Medical Oncology, University Medical Center Utrecht, Utrecht University, Utrecht, the Netherlands. [2]Center for Translational Immunology, University Medical Center Utrecht, Utrecht University, Utrecht, the Netherlands. [3]Princess Máxima Center for Pediatric Oncology, Utrecht, the Netherlands. [4]Department of Epidemiology, Julius Center for Health Sciences and Primary Care, University Medical Center Utrecht, Utrecht University, Utrecht, the Netherlands. [5]Department of Gastroenterology, University Medical Center Utrecht, Utrecht University, Utrecht, the Netherlands. [6]These authors contributed equally: Karijn P. M. Suijkerbuijk, Femke van Wijk. *A list of authors and their affiliations appears at the end of the paper. e-mail: f.vanwijk@umcutrecht.nl

steroids and/or initiation of second-line immunosuppression are recommended[2–4].

Data from our group illustrate that the current empirical approach is not optimal, as we showed that both high peak-dose steroids and second-line immunosuppression are independently associated with worse overall and cancer-specific survival in patients with melanoma treated for irAEs[5–8]. These findings warrant investigation of alternative strategies to limit cumulative exposure to immunosuppressants by timely introducing tailored second-line agents or skipping steroids dose escalation treatments. On the other hand, we currently lack mechanistic cues and clinical predictors for steroid unresponsive types of inflammation, which is urgently required to design personalized alternative treatment regimens[1].

Here, we apply a multi-omics approach to find blood- and tissue-based predictors for response to steroids, longitudinally evaluate effects of steroids in peripheral blood immune responses and explore potential mechanisms driving steroid non-response in, especially gastro-intestinal, irAEs. We find clear trends for elevated Th1/Th17-associated immune responses in blood and tissue of patients with irAEs not responding to steroids alone. On the contrary, cross-sectional analysis of colitis tissue suggests rapid effects of steroids on lymphocyte infiltration in steroid responders. Our findings can help in early identification of patients with irAEs requiring second-line immunosuppression and may guide second-line treatment strategies in steroid non-responders.

Methods

Patient selection, sample collection and outcome definition

Peripheral blood mononuclear cell (PBMC), serum and snap-frozen colon biopsies from patients enrolled in the UNICIT biobank study were included. In this biobank study, adult patients undergoing immune checkpoint inhibitor treatment for solid malignancies at University Medical Center Utrecht are enrolled and blood and stool samples are collected early during treatment, upon onset of irAEs and after each line of immunosuppressive treatment for irAEs, together with biopsies in case of diagnostic procedures. Details of the UNICIT cohort have been described previously[9].

For the present study, PBMC samples were selected for flow cytometry from UNICIT patients that developed clinically relevant irAEs, defined as CTCAE grade ≥2 and requiring ≥0.5 mg/kg/day corticosteroids. Moreover, the selection was enriched for melanoma (75%) and gastro-intestinal toxicity (75%), with paired samples before and after initiation of systemic steroids available (Table 1). The extended serum cohort consisted of serum samples from all patients in the flow cytometry cohort, supplemented with extra pre-steroids-only samples from UNICIT patients treated with systemic steroids for irAEs, again enriched for melanoma (77.5%) and gastro-intestinal toxicity (80.0%; Table 2). Patients with simultaneous gastro-intestinal infections were excluded. For bulk RNA-sequencing, all snap-frozen colon biopsies from UNICIT patients with histologically confirmed ICI colitis who required immunosuppressive treatment were selected (Supplementary Table 1). Digital images of hematoxylin & eosin (H&E) colon tissue slides from patients included for bulk RNA-seq were also used, along with H&E images from patients diagnosed with ICI colitis selected from a retrospective registry containing patients with ICI colitis treated at University Medical Center Utrecht until January 2023 (Supplementary Table 2). Healthy donor blood (for PBMCs) was obtained from the University Medical Center Utrecht Mini Donor Service.

Blood was collected in sodium heparin tubes for PBMCs and clot-blood tubes for serum. PBMCs were isolated with Ficoll-Paque density-gradient centrifugation (GE Healthcare), frozen in RPMI-1640 medium (Gibco) with 2 mM L-glutamine (Gibco), 100 IU/ml penicillin/streptomycin (Gibco), 20% fetal bovine serum (FBS; Invitrogen) and 10% dimethylsulfoxide and stored at −196 °C. Serum was isolated and frozen at −80 °C within 4 h of blood collection. Colon biopsies in the RNA-seq cohort and retrospective registry were obtained during flexible sigmoidoscopy (81%) or full colonoscopy (19%) with pinch biopsy forceps from macroscopically inflamed mucosa, or at random if no macroscopic abnormalities were present. Biopsies for RNA-seq were snap-frozen in liquid nitrogen immediately after collection and stored at −80 °C.

Steroid non-responders were defined as patients requiring any second-line immunosuppression to achieve complete remission of irAEs before steroids had been fully tapered.

Spectral flow cytometry

Cells were thawed and plated at ~1.0–3.0 × 10^6 per well for spectral flow cytometry. Cells were first restimulated with 20 ng/ml phorbol 12-myristate 13-acetate (PMA; Sigma-Aldrich) and 1.0 µg/ml ionomycin (Sigma-Aldrich; 4 h, 37 °C, 5% CO_2), with GolgiStop (0.26% monensin; BD Biosciences, 1:1500) added for the last 3.5 h. Cells were stained with fixable viability dye eFluor506 (Invitrogen; 30 min, 4 °C), washed and then stained with the surface mix (Supplementary Table 3) in FACS buffer (phosphate buffered saline [PBS, Sigma-Aldrich], 2% FBS, 0.1% sodium azide; 25 min, 4 °C). Cells were fixed and permeabilized with the eBioscience FoxP3/transcription factor fixation/permeabilization kit (Invitrogen) for 30 min at 4 °C, followed by the intracellular/intranuclear mix (Supplementary Table 3) in permeabilization buffer (30 min, 4 °C). Cells were kept in the dark at 4 °C until the next day and were then measured on a Cytek® Aurora™ 5 L spectral flow cytometer. Cytek® FSP™ CompBeads were used for all single-stain controls, except for CD8, CD45RA and TNF-α, which were prepared with cells. Unstained controls were prepared with cells from each individual measured. Bridging controls from one patient and one healthy donor were taken along in all three batches. Before measurement, daily quality control was performed with SpectroFlo QC beads. Samples were randomized over different batches by response to steroids (primary outcome) and longitudinal samples from the same subject were included in the same batch and measured consecutively.

After spectral unmixing with SpectroFlo software (Cytek), FlowJo (Tree Star) was used to pre-gate live singlets (Supplementary Fig. 1). Further analysis was exclusively performed in R and based on a published pipeline[10]. First, data were archsinh-transformed with cofactor=6000 for all channels except FSC/SSC and quality control was performed with the *peacoQC* package (IT_limit = 0.55, MAD = 6)[11]. After pre-gating and quality control, over 22 million cells remained for further analysis. Batch effect and intra-patient variation not attributable to biology was corrected by a custom landmark-based normalization method similar to fdaNorm[12], but using the downslope infliction point instead of density maxima as landmarks.

Next, data were clustered using a combination of *FlowSOM* and *Seurat*. To this end, data were first centered log ratio (CLR) normalized and then clustered with *FlowSOM* (nClus=50)[13] based on CD57, CD56, FoxP3, CD161 (KLRB1), CD39, CD3, CD16, CCR7, HLA-DR, CD4, CD8, CD14 and CD45RA to identify immune cell subsets present within the PBMC fraction. Subsequently, we visualized cell clustering in two-dimensional space using *Seurat*[14]. To this end, we randomly drew a 1% subset (~ 220,000 cells) of the complete data set. Data were CLR-normalized and scaled with *ScaleData()*, followed by principal component analysis (PCA), Uniform Manifold Approximation and Projection (UMAP) and clustering with *FindNeighbors()* based on FSC/SSC along with the same markers used for the Self-Organizing Map (FlowSOM). Optimal clustering resolution was assessed with *Clustree*[15]. Major subsets were identified by grouping together similar FlowSOM-clusters (Supplementary Fig. 2a). FlowSOM metacluster 1 (containing 0.018% of all cells) was discarded, because it contained outlier events with 21 (biologically unrelated) markers showing extremely high expression compared to other metaclusters, suspect for residual debris. Next, abundance of cell subsets and their functional profiles was assessed by analyzing expression levels of cytokines, receptors and transcription factors.

PD-1 receptor occupancy assay

T cell fractions completely or partially bound by PD-1-blocking therapeutic antibodies were estimated using a previously described receptor occupancy assay[16]. Briefly, in this approach cells are stained both with anti-PD-1 clone EH12.1, competitive with nivolumab and pembrolizumab, and with anti-human IgG4 (specifically binding nivolumab or pembrolizumab). For this

Table 1 | Flow cytometry PBMCs cohort

		Steroid responder (*N* = 13)	Steroid non-responder (*N* = 11)	Healthy donor (*N* = 6)
Female sex, *n* (%)		4 (30.8%)	6 (54.5%)	4 (66.7%)
Median age, yr (IQR)		61 (58-70)	67 (59-70)	62 (61-63)
Tumor type, *n* (%)	melanoma	9 (69.2%)	9 (81.8%)	
	non-small cell lung cancer	1 (7.7%)	2 (18.2%)	N/A
	renal cell carcinoma	3 (23.1%)	0 (0.0%)	
Tumor stage IV, n (%)		12 (92.3%)	8 (72.7%)	N/A
ICI Treatment, n (%)	ipilimumab monotherapy	0 (0.0%)	1 (9.1%)	
	ipilimumab + nivolumab	10 (76.9%)	6 (54.5%)	N/A
	anti-PD-(L)1 monotherapy	3 (23.1%)	4 (36.4%)	
Main irAE type, n (%)	colitis	5 (38.5%)	8 (72.7%)	
	gastritis/duodenitis	3 (23.1%)	2 (18.2%)	
	hepatitis	3 (23.1%)	1 (9.1%)	N/A
	pneumonitis	1 (7.7%)	0 (0.0%)	
	encephalitis	1 (7.7%)	0 (0.0%)	
Main irAE CTCAE grade, n (%)	II	4 (30.8%)	3 (27.3%)	
	III	9 (69.2%)	7 (63.6%)	N/A
	IV	0 (0.0%)	1 (9.1%)	
≥1 concomitant irAE(s), n (%)		5 (38.5%)	5 (45.5%)	N/A
(Systemic) steroid use at ICI initiation	N (%)	1 (7.7%)	2 (18.2%)	N/A
	Mean daily dosage (mg dexamethasone)	4	2.5	N/A
Median time from ICI initiation to patient-reported irAE symptom onset, days (IQR)		41 (34–69)	23 (14–82)	N/A
Median time from irAE symptom onset to steroid initiation, days (IQR)		7 (1–11)	1 (0–5)	N/A
Start dose prednisone, *n* (%)	0.5 mg/kg	0 (0.0%)	1 (9.1%)	
	1.0 mg/kg	9 (69.2%)	3 (27.3%)	N/A
	2.0 mg/kg	4 (30.8%)	7 (63.6%)	
Underwent prednisone dose escalation, *n* (%)	All to 2.0 mg/kg	3 (23.1%)	3 (27.3%)	N/A
Median time between pre-steroids sample collection and steroids initiation, days (IQR)		2 (0–3)	0 (0–2)	
Median time between pre- and post-steroids sample, days (IQR)		15 (9–28)	6 (5–12)	N/A

CTCAE denotes 'Common Terminology Criteria for Adverse Events', *ICI* 'immune checkpoint inhibitor', *irAE* 'immune-related adverse event', *yr* 'year'. Concomitant irAEs (*n*) include colitis/diarrhea (2), dermatitis (1), encephalitis (1), enteritis (1), hepatitis (5), hyperthyroidism (1), meningitis (1), polyneuropathy (1).

assay, 1.0×10^6 cells were plated and stained, fixed and permeabilized similarly to the spectral flow cytometry protocol, but now after 5 h incubation (37 °C, 5% CO_2) in presence of GolgiStop (1:1500), without PMA/ionomycin, to enable measurement of CXCL13[17], and using the staining mix in Supplementary Table 4. Cells were measured the next day on an LSR Fortessa. Data were analyzed in FlowJo according to the gating strategy in Supplementary Fig. 1.

ICI-bound PD-1 internalization assay

Pre-steroids PBMCs from 4 patients (2 with highest $CD4^+$ T cell PD-1 RO and 2 with lowest $CD4^+$ T cell PD-1 RO) were stained with the staining mix in Supplementary Table 5 as described above, but this time immediately after thawing. Each patient sample was then split in three and each aliquot was measured on an ImageStream X Mark II at 0, 30 and 60 min after completion of staining, to assess internalization of ICI-bound PD-1 receptor over time in the ex vivo situation. Internalization was quantified by the internalization feature, derived from the ratio of intracellular-to-total-cell intensity of PE (IgG4), using the Internalization Wizard in IDEAS software. The standard deviation of the Internalization feature was approximated by 1.25 × MAD (median absolute deviation).

Serum multiplex immunoassay

Serum concentrations of 26 analytes (IL-5, IL-6, IL-10, IL-12, IL-13, IL-17, IL-21, IL-23, TNF-α, IFN-γ, APRIL, CCL2, CCL4, CCL17 [TARC], CXCL9, CXCL10, CXCL13, CD40L, soluble IL-2Rα, granzyme B, TGF-β1, TACI, galectin-9 [Gal9], MMP-3, MMP-9 and MMP-10) were measured using an in-house developed and validated (ISO9001 certified) multiplex immunoassay (Center for Translational Immunology, University Medical Center Utrecht) based on Luminex technology (xMAP, Luminex Austin TX USA). The assay was performed as described previously[18]. A-specific heterophilic immunoglobulins were preabsorbed from all samples with heteroblock (Omega Biologicals, Bozeman MT, USA). Acquisition was performed with the Biorad FlexMAP3D (Biorad laboratories, Hercules USA) in combination with xPONENT software version 4.2 (Luminex). Data was analyzed by 5-parametric curve fitting using Bio-Plex Manager software, version 6.1.1 (Biorad).

Bulk RNA-sequencing

RNA isolation. RNA isolation was performed using the RNeasy Mini kit (Qiagen). First, 2 mL microcentrifuge tubes containing a 5 mm stainless steel bead (Qiagen) were precooled on dry ice, while the adapter of the

Table 2 | Extended serum cohort

		Steroid responder (*N* = 14)	Steroid non-responder (*N* = 17)
Female sex, *n* (%)		7 (50.0%)	9 (52.9%)
Median age, yr (IQR)		69 (60-72)	58 (52–71)
Tumor type, *n* (%)	melanoma	8 (57.1%)	14 (82.4%)
	non-small cell lung cancer	1 (7.1%)	1 (5.9%)
	squamous cell carcinoma	0 (0.0%)	1 (5.9%)
	urothelial cell carcinoma	1 (7.1%)	0 (0.0%)
	renal cell carcinoma	4 (28.6%)	0 (0.0%)
	melanoma, NSCLC, mesothelioma	0 (0.0%)	1 (5.9%)
Irresectable tumor stage III and IV, *n* (%)		14 (100.0%)	16 (94.1%)
ICI Treatment, *n* (%)	ipilimumab + nivolumab	12 (85.7%)	13 (76.5%)
	anti-PD-1 monotherapy	1 (7.1%)	2 (11.8%)
	anti-PD-1 + targeted/chemotherapy	1 (7.1%)	2 (11.8%)
Main irAE type, *n* (%)	colitis	8 (57.1%)	12 (70.6%)
	gastritis/duodenitis	2 (14.3%)	4 (23.5%)
	hepatitis	4 (28.6%)	0 (0.0%)
	ileitis terminalis	0 (0.0%)	1 (5.9%)
Main irAE CTCAE grade, *n* (%)	II	8 (57.1%)	8 (47.1%)
	III	6 (42.9%)	9 (52.9%)
≥1 concomitant irAE(s), *n* (%)		6 (42.9%)	7 (41.2%)
(Systemic) steroid use at ICI initiation	*N* (%)	1 (7.1%)	2 (11.8%)
	Mean daily dosage (mg dexamethasone equivalence*)	4	2.75
Median time from ICI initiation to patient-reported irAE symptom onset, days (IQR)		25 (21-40)	47 (29−63)
Median time from irAE symptom onset to steroid initiation, days (IQR)		2 (0–4)	5 (4–8)
Start dose prednisone, *n* (%)	0.5 mg/kg	1 (7.1%)	0 (0.0%)
	1.0 mg/kg	5 (35.7%)	10 (58.8%)
	2.0 mg/kg	8 (57.1%)	7 (41.2%)
Underwent prednisone dose escalation, *n* (%)	All to 2.0 mg/kg	1 (7.1%)	8 (47.1%)
Median time between pre-steroids sample collection and steroids initiation, days (IQR)		0 (0–1)	0 (0–1)

CTCAE denotes 'Common Terminology Criteria for Adverse Events', *ICI* 'immune checkpoint inhibitor', *irAE* 'immune-related adverse event', *NSCLC* 'non-small cell lung cancer', *yr* 'year'. Concomitant *irAEs* (*n*) include cholangitis (1), colitis (2), gastritis (5), hepatitis (4), nephritis (1), pancreatitis (1), pneumonitis (1), thyroiditis (1). * 1 patient used 10 mg prednisone daily for polymyalgia rheumatica, which was converted to 1.5 mg dexamethasone equivalence.

TissueLyser LT (Qiagen) was placed on regular ice. After 15 min, frozen biopsies were transferred into the 2 mL tubes and placed in the adapter, 600 µL Lysis buffer per sample (containing 10 µL β-mercaptoethanol per mL RLT buffer) was added and the TissueLyser was switched on as quickly as possible for disruption and homogenization (total 6 cycles × 1 min, 25 Hz). In between cycles, the tissue adapter containing the samples was cooled on regular ice for 30 s. Next, tubes were briefly centrifuged to remove foam and debris from the lids (5 sec., 13,000 rpm, RT). The lysates were pipetted into new Eppendorf tubes and centrifuged (3 min, 13,000 rpm, RT). The supernatant was transferred into new 1.5 mL tubes without debris or pellet, to which 0.5× volumes of 70% ethanol were added and then lysates were transferred to the RNeasy spin columns. Next steps of the RNeasy Mini kit were performed according to the manufacturer's protocol. This homogenization and RNA isolation protocol yielded optimal and balanced RNA quantity, purity and quality (measured by an Implen N60/N50 NanoPhotometer and Agilent 2100 Bioanalyzer system using the Agilent RNA 6000 Pico Kit).

RNA sequencing. Library preparation was performed at GenomeScan with the NEBNext Ultra II Directional RNA Library Prep Kit (Illumina) according to protocol NEB #E7760S/L and included mRNA isolation by oligo-dT magnetic beads. Sufficient quality and yield for all samples before sequencing was verified on a Fragment Analyzer (Agilent). Twenty-million paired-end (150 bp) reads per sample were sequenced on a NovaSeq 6000 sequencer. Reads were then trimmed with *fastp* v0.23.5, mapped to a human reference genome (GRCh38.p13) based on Burrows-Wheeler Transform (STAR2 v2.7.10) and count tables were created with *HTSeq* v2.0.2. Transcripts-per-million (TPM) values were calculated with *Cufflinks* v2.2.1.

Bulk RNA-seq analysis. Low-abundant genes (total ≤ 5 counts or ≤ 0.01 TPM across samples) were filtered. Absolute abundance estimates of 22 immune cell subsets were deconvoluted with the CIBERSORT algorithm in absolute mode using the LM22 signature matrix and untransformed TPM files[19]. Only samples deconvoluted at $P_{perm} < 0.05$ were kept for further analysis. We additionally leveraged the LM7 signature mix in an attempt to obtain more reliable estimations of γδ T cells[20], given their high expected abundance in colonic mucosa. However, LM7 and LM22 results with respect to γδ T cells were similar and therefore, we exclusively used LM22 results. Gene set variation analysis (GSVA) was performed with

GSVA v1.52.3[21], using logTPM values. We measured the bMIS_UC gene set (Supplementary Table 6), validated in ulcerative colitis to molecularly assess mucosal inflammation and predict treatment outcome[22]. In addition, a published Th17.1 gene signature[23] and custom gene sets were analyzed, deliberately containing mutually exclusive Th1-, Th2- and Th17-related genes (Supplementary Table 6) to maximize any signal for immune skewing. A core signature for mature B cells and plasma cells was compiled based on human scRNA-seq results[24].

Pooled single-cell transcriptomic data meta-analysis

$CD4^+$ and $CD8^+$ T cell transcriptomic data from 37 patients with ICI colitis (70.3% steroid-naïve upon endoscopy) for whom response to steroids was reported from three single-cell RNA-sequencing studies were reanalyzed with *Seurat*[25–27]. Non-responders were defined as patients who were reported to have received second-line immunosuppressive therapy after steroids.

From the Thomas et al. dataset (GEO: GSE206301)[25], patients of interest were selected from T cell transcriptomic data provided in H5ad format. Separate Seurat objects were created for individual patients, only cells with 200-3,000 features and <10% mitochondrial RNA were kept and TCR genes were silenced[28]. The dataset was split by patient, *SCTransform()* with *glmGamPoi* was run on individual Seurat objects and then data from all patients were merged again. From the Gupta et al. dataset (GEO: GSE189040)[27], patients of interest could be directly selected from a Seurat object containing clustered and annotated T cell populations. From the Luoma et al. dataset (GEO: GSE144469)[26], $CD3^+$ sorted transcriptomic data were transformed as Seurat object and subjected to quality control and *SCTransform()* as outlined above. Variable features ($n = 3000$) were selected with *SelectIntegrationFeatures()*, followed by dimensionality reduction (*RunPCA()*, *RunUMAP()* with the first 30 dimensions) and clustering (*FindNeighbors()* with first 30 dimensions and *FindClusters()* at resolution = 1.0).

Next, only features detected in all three datasets were kept and all datasets were merged and clustered as described above. Cells were clustered again and mapped as unintegrated UMAP plot to evaluate the extent of study-derived batch effect. The original three datasets were then merged again, subjected to *SCTransform()* and PCA, followed by *IntegrateLayers()* using SCT-transformed data and reciprocal PCA (RPCA)[14]. Dimensionality reduction and clustering was repeated using integrated dimensions. Cluster-defining markers were identified with *FindAllMarkers()* and cell fractions per T cell cluster were calculated for all patients. Clusters were not individually annotated, but Th17 and Th22 clusters were specifically identified based on *IL17A* and *IL22* expression. GSVA was performed on pseudobulk data generated with *AverageExpression()* using SCT data. Differential gene expression was performed with *DESeq2* using pseudobulk data from raw RNA counts, adjusting for GSE dataset of origin[29].

Automatic nucleus segmentation and cell type classification in colitis H&E slides

Whole slide images of hematotoxylin & eosin (H&E) stained colon specimens were analyzed using the Hover-NeXt model trained on the Lizard dataset[30,31]. This model, trained with nuclei annotations from normal colon tissue and colorectal cancer, segments and classifies all visible nuclei into connective tissue nuclei, epithelial nuclei, neutrophils, eosinophils, plasma cells or lymphocytes. Next, tissue containing areas were manually annotated using QuPath[32]. These tissue annotations were used to filter out false positive nuclei annotations outside tissue area using the GeoPandas package. This resulted in a .GEOjson file with coordinates and classifications of nuclei inside the tissue area which was used for further analysis[33].

Statistics and Reproducibility

All analyses were performed in R v4.4.1. Median follow-up time was estimated with the reverse Kaplan-Meier method using the *survival* package. Unless otherwise specified, continuous variables between two or more than two groups were analyzed by Wilcoxon or Kruskal-Wallis tests without formal post-hoc test, respectively. Correlations were analyzed by Spearman's correlation. *P* values were adjusted for multiple testing with Benjamini-Hochberg procedures. Unadjusted *P* values were also reported given increased type II error rates with multiple-testing correction, to address the hypothesis-generating nature of this study. The alpha level was set to 0.05 and all tests were performed two-sided. Linear regression models were fit to quantify the relation of cell subsets with steroid response adjusted for ICI treatment type and *vice versa* with the *stats* package. Trends in cross-sectional data across different timepoints were visualized with local regression using locally estimated scatterplot smoothing (LOESS) embedded in *geom_smooth()* within *ggplot2*, with timepoints beyond 7 days winsorized. In boxplots, the box represents the interquartile range (IQR) and whiskers represent the absolute minimum of either a) 1.5×IQR, or b) the extreme value of a collection of data points. Mentioned sample sizes reflect the number of unique patients enrolled in an experiment, unless otherwise specified.

Ethics

The UNICIT biobank study was not considered subject to the Dutch Medical Research with Human Subjects Law by the medical research ethics committee of the University Medical Center Utrecht. The UMC Utrecht biobank review committee approved the UNICIT biobank protocol (TCbio 18-123) and granted permission for use of human biospecimens for this study (TCbio 23-200). All participants in this biobank study provided written informed consent in line with de Declaration of Helsinki. Informed consent was waived for the use of data from patients who had not opted-out for use of their health data for research purposes and who had been included in a single-center retrospective colitis registry.

Results

In March 2024, a total of 535 patients had been prospectively enrolled in the UNICIT biobank, which includes patients with solid tumors undergoing ICI treatment at University Medical Center Utrecht, the Netherlands[9]. During a median follow-up of 23.6 months (95% confidence interval [CI]: 20.4-26.2), 156 unique patients developed 197 grade ≥2 irAEs requiring ≥0.5 mg/kg/day corticosteroids. Of those 156 patients, blood was collected at the onset of irAEs before initiation of immunosuppressive treatment in 87 patients (55.8%). Response to steroids and subsequent treatment lines for irAEs was recorded for all patients. Steroid non-responders can be categorized as steroid-resistant, steroid-refractory or steroid-dependent, depending on their initial response to steroids and relapse of symptoms upon steroid tapering[34,35]. In this study, we considered patients "steroid non-responders" when they required any second-line immunosuppression to achieve complete remission of irAEs before steroids had been fully tapered. A complete overview of the study design, including number and type of samples used and analyses performed, is in Fig. 1.

From all UNICIT patients who received ≥0.5 mg/kg/day corticosteroids for irAEs, we first selected patients with paired peripheral blood mononuclear cells (PBMC) and serum samples prior to and following initiation of steroids for irAEs, enriching for patients with gastro-intestinal irAEs (Table 1). We assessed abundance and functional phenotypes of immune cell subsets with spectral flow cytometry in pre- and on-steroids samples together. Annotation of 50 unsupervised clusters yielded 15 peripheral blood immune cell subsets (Fig. 2a) (Supplementary Fig. 2a).

Blood- and tissue-based prediction of steroid response

We first aimed to identify predictors for steroid response in blood by analyzing pre-steroids samples only, collected median 1 day (IQR: 0-3 days) before initiation of steroids. At irAE onset, before steroids had been initiated, none of the 15 immune cell subsets predicted steroid response (Fig. 2b), irrespective of ICI type (Supplementary Fig. 2b, c). We then focused on different T cell subsets, by assessing expression of functional markers in original unsupervised clusters (Fig. 2c for $CD8^+$ T cells) (Supplementary Fig. 2d for $CD4^+$ T cells). None of the detailed T cell clusters was predictive of steroid non-response after multiple testing correction. However, based on

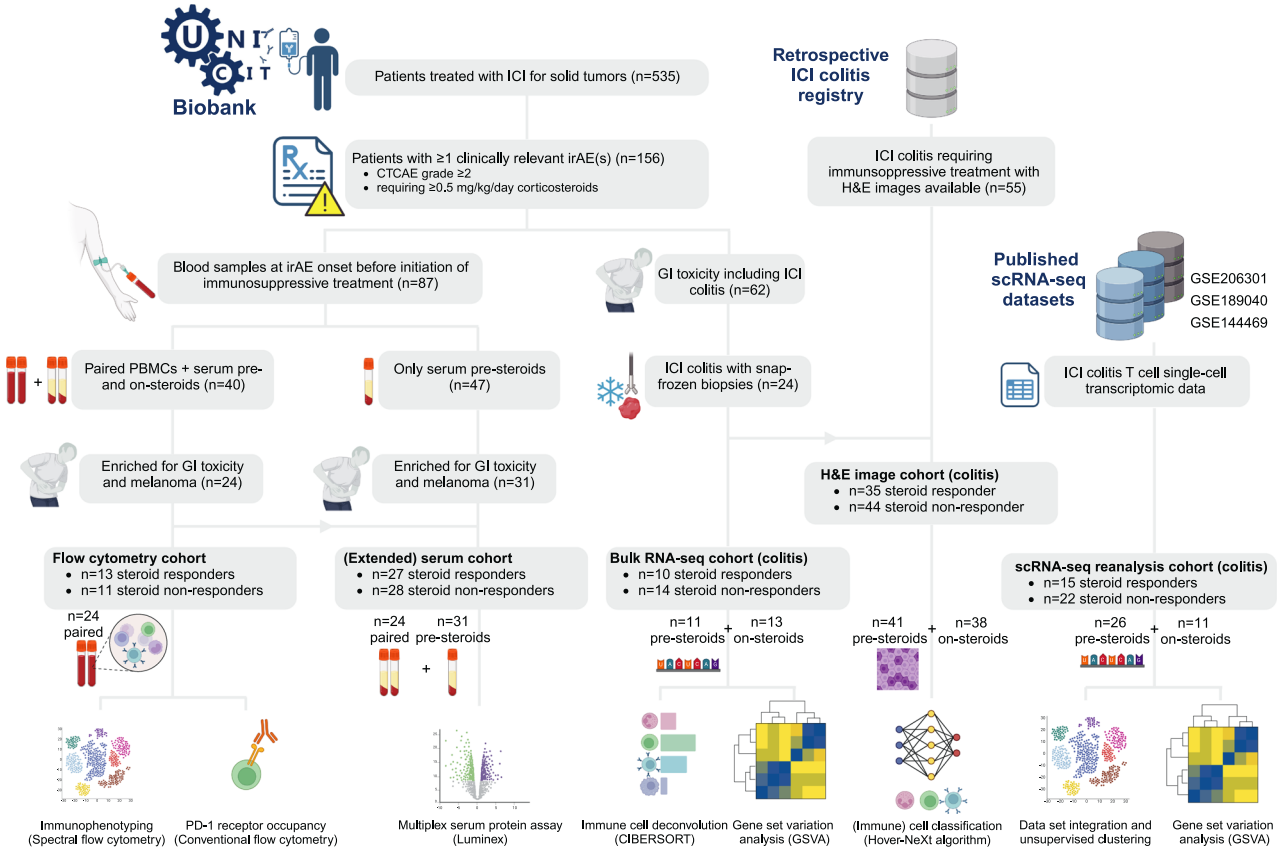

Fig. 1 | Study design. Overview of patients included in this study, type and number of samples used and the sources for all samples and data. For all patients (samples), the response to steroids and timing of sampling (pre-steroids, on-steroids or paired pre- and on-steroids) is shown. Abbreviations: CTCAE denotes 'Common Terminology Criteria for Adverse Events', GI 'gastro-intestinal', H&E 'hematoxylin and eosin', ICI 'immune checkpoint inhibitor', irAE 'immune-related adverse event'. In the RNA-seq and H&E cohorts, pre- and on-steroids samples were not paired, but for each patient either a pre- or an on-steroids sample was available. Proportions of pre- versus on-steroids samples were not statistically different between steroid responders and non-responders (Supplementary Tables 1–2). Detailed patient characteristics are in Tables 1–2 and Supplementary Tables 1–2. Created in BioRender. Van Eijs, M. (2024) https://BioRender.com/a21j801.

unadjusted *P* values, a trend for relatively higher $CD8^+$ Tem cluster 1 (Tc17-like; $IL17A^{hi}IFN\text{-}\gamma^{hi}$ but granzyme B^{lo}) and $CD8^+$ Tem cluster 3 (activated, proliferative, cytotoxic Tc1-like, equipped for gut homing; integrins $\beta1/\beta7^{hi}$ [36], granzyme $B^{hi}IFN\text{-}\gamma^{hi}Ki67^{hi}CD38^{hi}HLA\text{-}DR^{hi}$ but $IL17A^{lo}$), and lower exhausted $CD8^+$ T_{EMRA} cluster 3 ($PD\text{-}1^{hi}LAG\text{-}3^{hi}TIM\text{-}3^{hi}$ but granzyme $B^{lo}IFN\text{-}\gamma^{lo}TNF\text{-}\alpha^{lo}$) in steroid non-responders was found (Fig. 2d). These trends remained after adjustment for ICI type (Fig. 2e). Pre-steroids $CD4^+$ T cell clusters were not predictive of steroid response, but we could confirm our previous finding that ICI type was associated with the extent of $CD4^+$ effector memory proliferation (Supplementary Fig. 2e, f)[9]. Because our flow cytometry panels were dedicated to T cells, subsets of other potentially relevant cell types, including B cells and NK cells, could not be distinguished in same detail as T cells. However, when we ranked all 50 unsupervised clusters (Supplementary Fig. 2a) by their unadjusted significance level, NK cell clusters 6 ($CD16^{high}$ $CD56^+$), 4 and 14 (both $CD16^{dim}CD56^+$) comprised the top 4 clusters positively associated with steroid non-response, together with cluster 12 (an undefined cell cluster lacking expression of CD3, CD45RA, HLA-DR, CD39, CD14, CD16 and CD56), at $P_{raw} < 0.03$.

Subsequently, we measured serum concentration of 26 analytes in pre-steroids samples of the same patients, extended with pre-steroids samples obtained ≤4 days prior to steroids initiation from 31 extra patients (Table 2). In addition, complete blood counts with differential and C-reactive protein (CRP) concentrations were available from regular diagnostics in most patients. None of the analytes was differentially abundant pre-steroids in steroid non-responders compared to responders at $P_{adj} < 0.05$. Non-responders showed a trend of elevated (> 1.5×) serum interleukin (IL)-6, IL-17, IL-12, IL-23, matrix metalloproteinase-3 (MMP-3), MMP-10 and soluble IL-2-receptor (Fig. 2f). MMP-3 derives from various connective and visceral tissues and is strongly inducible by IL-17[37–39], suggesting type 17 skewing in tissue of non-responders. Serum IL-6 and CRP (induced among others by IL-6)[40], were correlated in the entire cohort ($r = 0.69$, $P = 6.6 \times 10^{-9}$ by Pearson's correlation). However, while mean IL-6 was numerically twofold higher in steroid non-responders than responders, (mean) pre-steroids CRP concentration was equal between both groups (Fig. 2g). Steroid responders, on the other hand, featured higher total leukocyte count (Fig. 2h), including elevated eosinophils, neutrophils and lymphocytes before initiation of steroids (Supplementary Fig. 2g–i). CRP levels correlated with leukocyte counts in steroid responders, but not in non-responders (Fig. 2i), which could indicate that IL-6 (and CRP) levels in steroid non-responders may be chronically elevated, whereas steroid responders feature more of an acute phase response with leukocytosis in parallel to (acute) CRP increases. The latter has been associated with favorable response to steroid treatment in inflammatory bowel disease (IBD)[41].

Finally, we selected all 24 patients from the biobank with histologically confirmed ICI colitis and snap-frozen biopsies obtained either before or after initiation of steroids (Supplementary Table 1). Bulk RNA isolated from whole colon biopsies was sequenced and absolute abundance of 22 immune cell types was deconvoluted with CIBERSORT[19]. First, we only analyzed samples from the 11 patients that were steroid-naïve at endoscopy and had sufficiently reliable deconvolution results (at $P_{permutation} < 0.05$). The distribution of pre- versus on-steroids samples was not associated with steroid response in the bulk RNA-seq cohort ($P = 0.23$ by Fisher's exact; Supplementary Table 1). Before initiation of

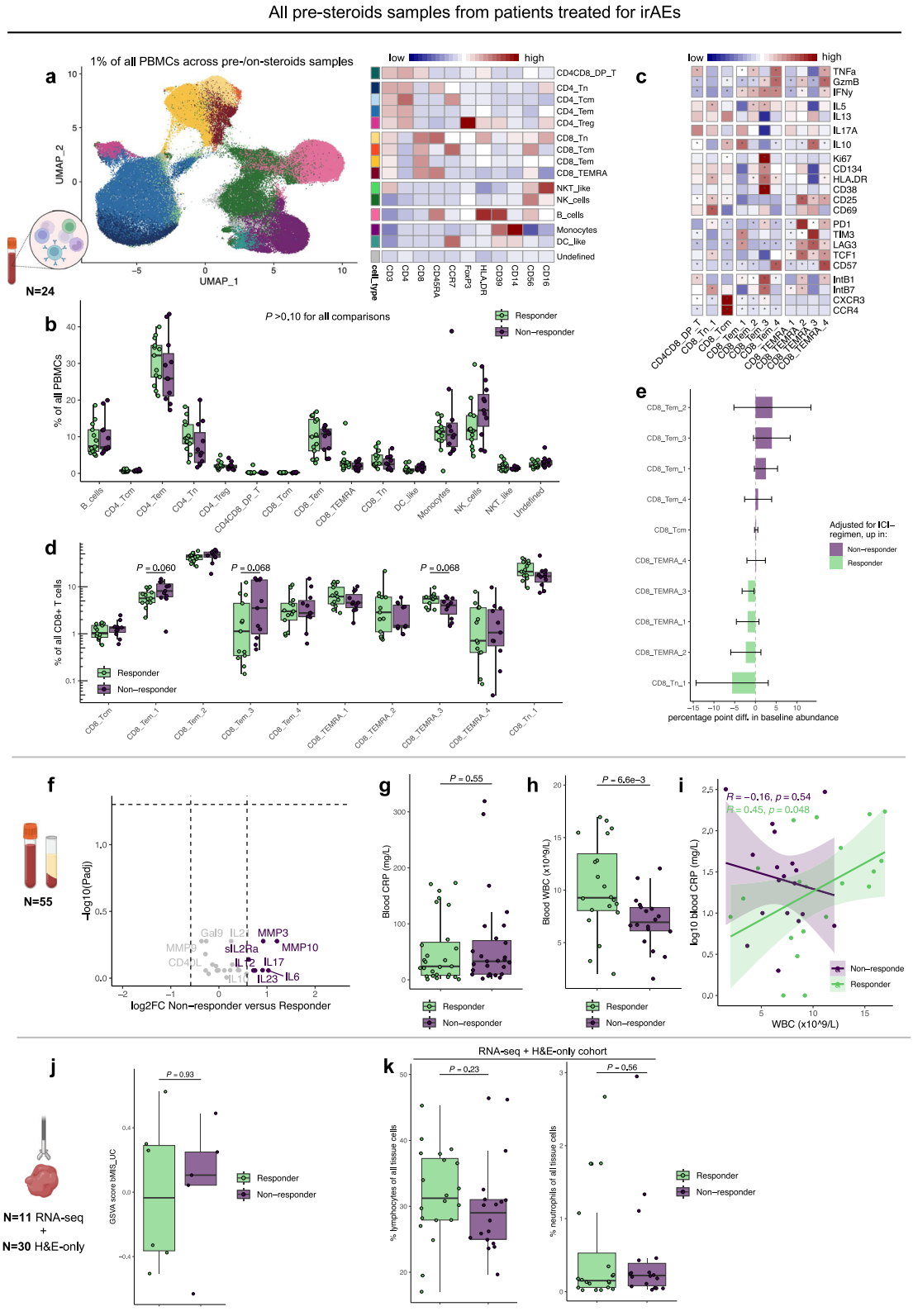

steroids, non-responders had more activated memory CD4$^+$ T cells in ICI-type-adjusted analysis (Supplementary Fig. 2j). Pre-steroids extent of mucosal inflammation was assessed molecularly by gene set variation analysis (GSVA) using a biopsy molecular inflammation score developed in ulcerative colitis (bMIS_UC)[22]. Higher bMIS_UC indicates more inflammation, but the bMIS_UC was not different between steroid responders and non-responders (Fig. 2j).

To accommodate the limited sample size of our preliminary analyses of snap-frozen tissue before steroids initiation, we extended this cohort with 55 ICI colitis patients (including 30 steroid-naïve patients) from whom digital images of hematoxylin and eosin (H&E) stained colon slides were available (Supplementary Table 2). Again, the proportion of pre- versus on-steroids samples was not associated with steroid response in the extended H&E cohort ($P = 0.59$ by Fisher's exact; Supplementary Table 2). Nuclei were

Fig. 2 | Blood- and tissue-based prediction of steroid response. Unadjusted *P* values are displayed, unless otherwise specified. **a** Clustering of PBMCs based on UMAP embeddings obtained in a 1% random subset of the entire dataset (including all time points), overlaid with annotated FlowSOM-based clusters, along with the expression heatmap displaying median expression of lineage-defining markers in FlowSOM-based clusters. For the lack of B-cell-specific markers, B cells were annotated by exclusion and based on HLA-DR, CD39 and CD45RA positivity. **b** Boxplots displaying pre-steroids abundance of PBMC subsets by response to steroids. Comparison by two-sided Wilcoxon test in $N = 24$ patients; unadjusted *P* values were >0.10 for all comparisons. **c** Expression heatmap displaying median expression of functional markers in $CD8^+$ T cell subsets, grouped from top to bottom as Th1-related, Th2-related, Th17-related, Immunosuppressive, Proliferation/activation, Dysfunction/exhaustion and Homing/trafficking. Except CD57 and HLA-DR, these markers were not used as clustering parameters in FlowSOM. * Significant marker enrichment at $P_{adj} < 0.05$. **d** Boxplots displaying pre-steroids abundance of $CD8^+$ T cell subsets by response to steroids. Comparison by two-sided Wilcoxon test in $N = 24$ patients; unadjusted *P* values are shown. **e** Relative pre-steroids abundance of $CD8^+$ T cell subsets by response to steroids, adjusted for ICI treatment type in $N = 24$ patients. Linear regression coefficients are shown with whiskers indicating 95% confidence intervals of coefficients. **f** Volcano plot displaying difference in pre-treatment concentration of 26 serum proteins measured by multiplex assay in responders versus non-responders in the full extended cohort. Boxplots displaying pre-treatment (**g**) C-reactive protein (CRP) and (**h**) blood leukocytes (WBC), by response to steroids in the full extended cohort. Comparisons by two-sided Wilcoxon tests in $N = 54$ (**g**) and $N = 38$ (**h**) patients (CRP and WBC were missing in 1 and 17 patients, respectively). **i** Scatter plot displaying (log_{10}) blood C-reactive protein (CRP) in relation to white blood cell (WBC) count, with two-sided Pearson's correlation with linear regression line and its 95% confidence interval separately for steroid-responders ($N = 20$) and non-responders ($N = 18$). Boxplots displaying pre-steroids (**j**) molecular inflammation assessed by gene set variation analysis using the bMIS_UC score and (**k**) percentages lymphocytes and neutrophils of all tissue cells, identified by HoVer-NeXt, in H&E slides of ICI colitis, by response to steroids. Comparisons by two-sided Wilcoxon test in $N = 11$ (**j**) and $N = 38$ (**k**) patients (percentages neutrophils and lymphocytes were missing for 3 patients in the RNA-seq cohort). Unadjusted *P* values are shown. Blood and tissue symbols in this figure created in BioRender. Van Eijs, M (2024) https://BioRender.com/a21j801.

segmented and connective tissue, epithelial cells, lymphocytes, plasma cells, neutrophils and eosinophils were annotated with the HoVer-NeXt algorithm specifically trained on colon tissue data[30]. When analyzing steroid-naïve samples only, no differences were observed in total lymphocyte or neutrophil infiltration in relation to steroid response (Fig. 2k).

In conclusion, no statistically significant associations between peripheral blood immune cell subsets or serum proteins and steroid response were found. However, non-response to steroids showed trends toward increased circulating percentages of Tc1- and Tc17-like $CD8^+$ T cells, as well as elevated serum IL-12, IL-23, IL-6 and IL-17 prior to initiation of steroids. In tissue, activated $CD4^+$ T cells, but not total lymphocytes, neutrophils or molecular inflammation were associated with steroid non-response.

Changes in blood and tissue after initiation of steroids in relation to response

To explore longitudinal differences in steroid responders versus non-responders, we analyzed the change in PBMC subsets and serum proteins in paired pre- and on-steroids samples. On-steroids samples were collected median 10 days (IQR: 6–17) after initiation of steroids, but before initiation of second-line immunosuppression in non-responders. Time between pre- and on-steroids samples was not significantly different between responders and non-responders (Table 1). No changes of cell subsets or serum proteins after initiation of steroids were observed upon multiple-testing correction (Fig. 3a-e, Supplementary Fig. 3a). However, based on uncorrected *P* values, we found trends for persistently high $CD8^+$ Tem cluster 3 (activated, proliferating Tc1-like) cells in steroid non-responders, whereas this cluster decreased median twofold in steroid responders (Fig. 3b, c). Based on unadjusted *P* values, longitudinal serum analysis showed trends between steroid non-response and persistently high or increasing levels of chemokines (C-X-C motif) ligand 10 (CXCL10), C-C motif (CC) ligand 4 (CCL4), CXCL13, A Proliferation-Inducing Ligand (APRIL) and MMP9 (Fig. 3d). Particularly CXCL13, associated with germinal center activity, and APRIL, indicative of B cell activation, showed increases after initiation of steroids in non-responders (Fig. 3e). Together, these data may suggest persistent ($CD8^+$) T cell activation and proliferation, germinal center activity and antibody responses in steroid non-responders.

Building on observations that anti-PD-1-bound T cells preferentially proliferate in the context of irAEs[27,42], we hypothesized that persistent activation and proliferation of peripheral blood T cells in non-responders would be indicated by a higher proportion of PD-1 receptor bound by therapeutic antibody. In contrast to our hypothesis, neither pre-steroids PD-1 receptor occupancy (RO), nor change in PD-1 RO after initiation of steroids was associated with steroid response (Fig. 3f) (Supplementary Fig. 3b). As expected, PD-1 was completely unbound in a patient with late-onset toxicity >200 days after the last dose of ICI (Fig. 3g) (Supplementary Fig. 3c). Surprisingly, PD-1 RO was lower in patients treated with combined ipilimumab plus nivolumab. Since combination ICI is associated with increased ($CD4^+$) T cell proliferation[9], we suspected that rapid turnover of (bound) PD-1 receptor complexes in cycling cells could potentially distort measurements of PD-1 RO. This was supported by lower (apparent) PD-1 RO with higher $CD4^+$ T cell proliferation (Fig. 3h). However, in a sensitivity analysis excluding one outlier with >50% $CD4^+$ T cell proliferation, the association between PD-1 RO and $CD4^+$ T cell proliferation was no longer significant (Spearman's $\rho = -0.37$, $P = 0.14$), and neither was the association between PD-1 RO and $CD8^+$ T cell proliferation (Supplementary Fig. 3d). Also, internalization of drug-bound PD-1 did not increase over time in patients with lowest compared to highest PD-1 RO (Supplementary Fig. 3e, f), although image-based internalization is difficult to quantify in lymphocytes for the little volume of cytoplasm relative to nucleus size (Supplementary Fig. 3e). Together, these findings suggest that peripheral PD-1 receptor occupancy does not reliably reflect clinical steroid response, and may be confounded by T cell proliferation, particularly in patients receiving combination ICI.

Next, we turned from blood to tissue and analyzed molecular inflammation and immune cell infiltration in colon biopsies from, respectively 24 (with bulk RNA-seq data) and 79 (with H&E histological images) ICI patients that underwent endoscopy at different timepoints before or after initiation of steroids. Bulk RNA-seq analyses were limited by small sample size, which only allowed descriptive analysis. While similar bMIS_UC inflammation scores were observed at baseline between steroid responders and non-responders, bMIS_UC inflammation scores observed one day after initiation of steroids were numerically lower in responders compared with non-responders, who exhibited high mucosal inflammation regardless duration of steroids (Fig. 4a). Notwithstanding inherent limitations in interpretation of these cross-sectional data, this may reflect the clinical observation that some ICI colitis patients report symptom improvement within several hours to a day after initiation of steroids. Since pre-steroids molecular inflammation scores are unknown for responders who underwent endoscopy the day after initiation of steroids, confounding by (lower) severity should be considered. However, all three responders who underwent endoscopy at day 1 after steroids had grade 3 colitis, necessitating immediate steroidal treatment before endoscopic evaluation. In the extended cohort, comprising all 79 ICI colitis patients treated with steroids, a similar pattern was observed, with significantly lower lymphocyte infiltration (but not neutrophil infiltration) in steroid responders within the first 24 h of treatment versus baseline (Fig. 4b).

In summary, no statistically significant differences in longitudinal blood and tissue analyses were found between steroid responders and non-responders. Trends indicate that peripheral blood ($CD8^+$) T cell proliferation and activation is dampened in steroid responders, at least within several days of treatment, but possibly sooner. Persistent T cell proliferation in non-responders could not be linked to the extent of PD-1 receptor occupancy.

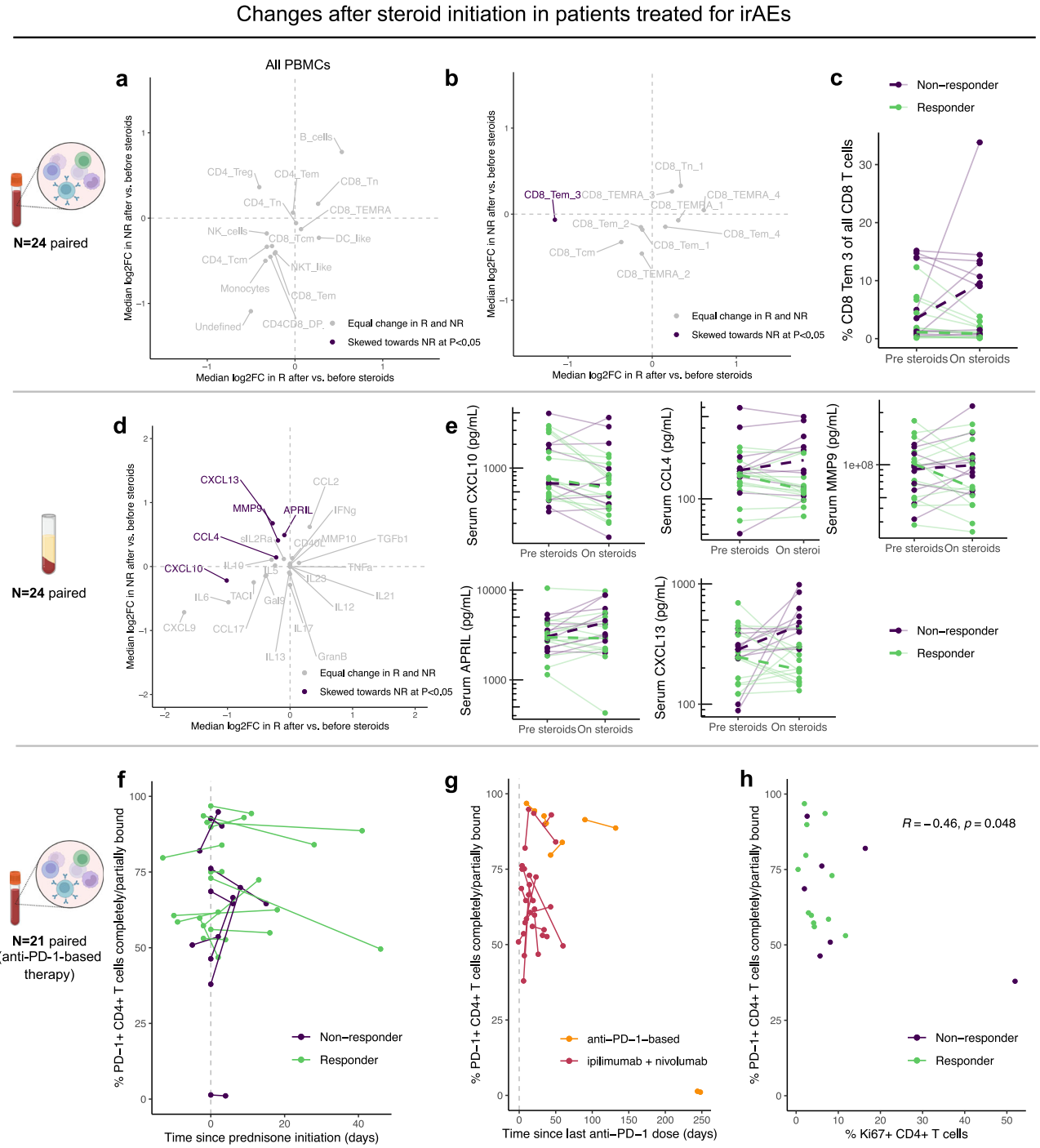

Fig. 3 | Changes in blood after initiation of steroids and PD-1 receptor occupancy in relation to steroid response. Median log_2 fold-change of (**a**) all PBMC and (**b**) $CD8^+$ T cell subsets after initiation of steroids, in steroid responders (R; x-axis) versus steroid non-responders (NR; y-axis). Unadjusted $P < 0.05$ for the difference in fold-change between responders and non-responders are indicated. "Skewing towards" an index group can constitute a relative increase in that index group, a relative decrease in the comparator group, or a combination of both. **c** Spaghetti plot displaying the change in $CD8^+$ Tem 3 cells for individual patients, colored by response to steroids. Dashed lines indicate median trends. **d** Same as (**a**,**b**), but displaying on-steroids change in serum protein concentration. **e** Same as (**c**), but displaying on-steroids change in CXCL10, CCL4, MMP9, APRIL and CXCL13. Scatter plots displaying the percentage of PD-1^+ $CD4^+$ T cells completely or partially bound by anti-PD-1 therapeutic antibody in relation to (**f**) duration of steroids or (**g**) time since last anti-PD-1 administration, by (**f**) response to steroids or (**g**) ICI treatment type, for paired pre-/on-steroids samples in $N = 21$ patients. No formal statistical tests were performed. **h** Scatter plot displaying the percentage of PD-1^+ $CD4^+$ T cells completely or partially bound by anti-PD-1 therapeutic antibody in relation to $CD4^+$ T cell proliferation for pre-steroids samples only. Analysis by two-sided Spearman's correlation in $N = 20$ patients (one patient with late-onset toxicity >200 days after the final ICI dose was excluded from this analysis). Blood symbols in this figure created in BioRender. Van Eijs, M. (2024) https://BioRender.com/a21j801.

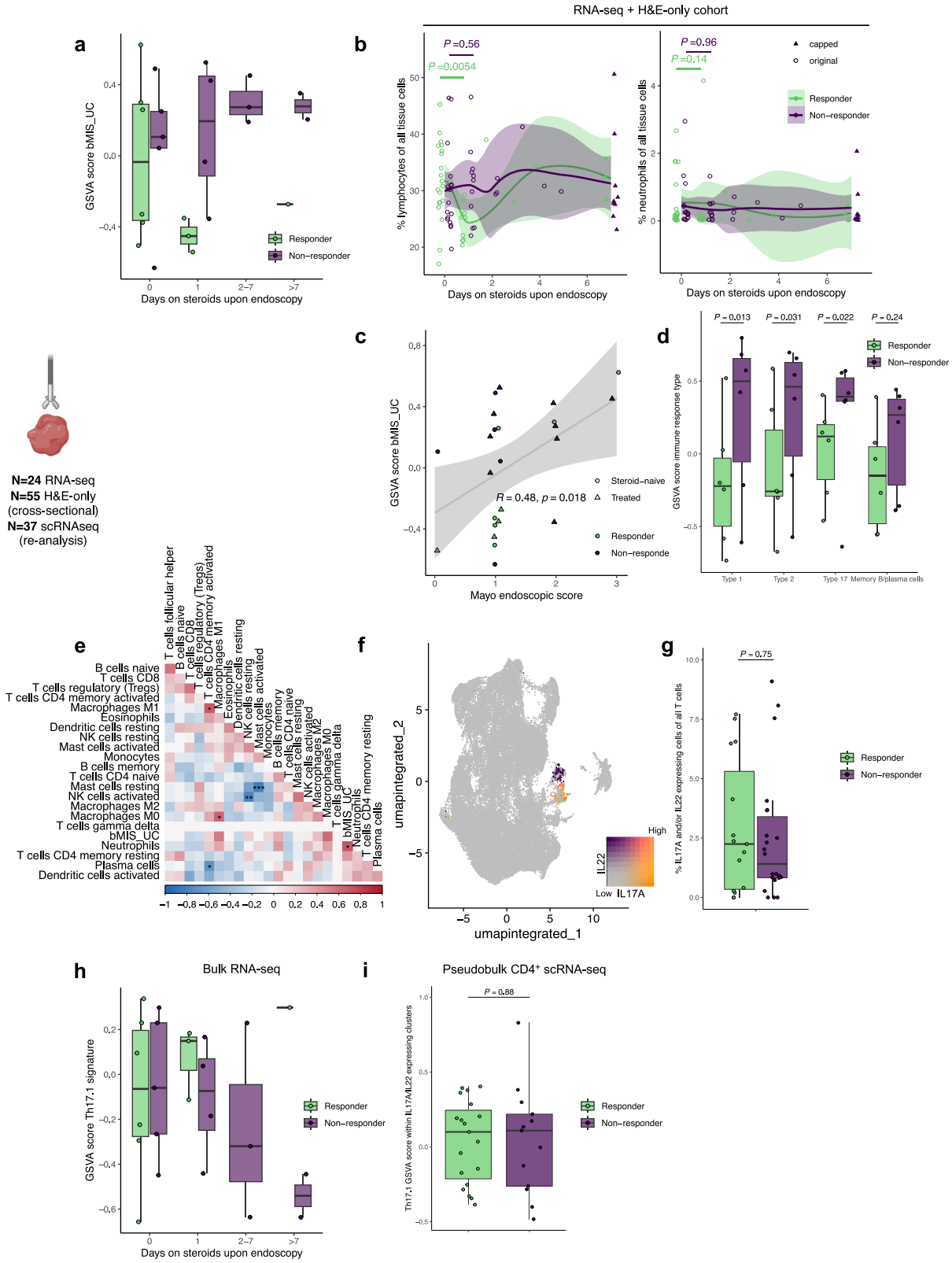

Trends in tissue data suggest that mucosal inflammation in ICI colitis may improve within 24 h after treatment initiation in steroid responders.

Exploration of mechanisms driving steroid non-response

Finally, we investigated immunological mechanisms in tissue underlying steroid response. Molecular inflammation correlated with the Mayo endoscopic score (MES), but provided a more granular impression of inflammation, particularly for endoscopically milder cases (Fig. 4c). Since activated CD4$^+$ T_{mem} cells were enriched in pre-steroids tissue of non-responders, we wondered if a specific T-helper response would underly steroid non-response. When using immunity-type-specific gene sets for GSVA in steroid-naïve and steroid-exposed biopsies combined, we found

Fig. 4 | Tissue correlates of steroid non-response and exploration of underlying mechanisms. Unadjusted *P* values are displayed, unless otherwise specified. **a** Boxplots displaying molecular inflammation assessed by gene set variation analysis using the bMIS_UC score, including all biopsies of patients treated with steroids, stratified by duration of steroids upon endoscopy. No formal statistical tests were performed. **b** Scatter plots of percentages lymphocytes and neutrophils of all tissue cells in relation to duration of steroids upon endoscopy, using all H&E slides from $N = 79$ ICI colitis patients treated with steroids. Trends in leukocyte infiltration in relation to duration of steroids are visualized by locally estimated scatterplot smoothing (LOESS). Datapoints with duration of steroids >7 days were winsorized at 7 days (indicated by solid triangles). Pre- versus 1-day on-steroids samples were compared by unpaired two-sided Wilcoxon tests, separately for steroid responders ($N = 29$) and non-responders ($N = 29$). **c** Scatter plot displaying molecular inflammation (by GSVA bMIS_UC score) in relation to Mayo endoscopic score in $N = 24$ patients, analyzed by two-sided Pearson's correlation with linear regression line and 95% confidence interval. **d** Boxplots displaying GSVA scores for three immune response type-specific and one memory B/plasma cell gene sets in all biopsies (pre- and on-steroids samples combined), stratified by steroid response group. **e** Two-sided Spearman's correlation matrix of 22 deconvoluted immune cell types and bMIS_UC score in all samples with sufficiently reliable deconvoluted compositions (at $P_{perm} < 0.05$); $^{*}P_{adj} < 0.05$, $^{**}P_{adj} < 0.01$, $^{***}P_{adj} < 0.001$. **f** UMAP visualization displaying *IL17A* and *IL22* expression in reanalyzed transcriptomic data of tissue $CD4^+$ and $CD8^+$ T cells in ICI colitis. **g** Boxplot displaying percentage *IL17A* and *IL22* expressing cells of all $CD4^+$ and $CD8^+$ T cells in same patients as (**f**), by response to steroids, analyzed by two-sided Wilcoxon test ($N = 37$). **h** Boxplots displaying Th17.1 signature enrichment in all bulk RNA-seq biopsies, stratified by requirement for immunosuppressive treatment and duration of steroids upon endoscopy. No formal statistical tests were performed. **i** Boxplots displaying Th17.1 signature enrichment in pseudobulk transcriptomic data of Th17/Th22 $CD4^+$ T cells, by response to steroids, analyzed by two-sided Wilcoxon test ($N = 37$). Tissue symbol in this figure created in BioRender. Van Eijs, M. (2024) https://BioRender.com/a21j801.

that type 1, type 2 and type 17 signatures were all significantly enriched in steroid non-responders, but type 1 and type 17 responses best differentiated between non-responders and responders (Fig. 4d). Additionally, neutrophils were the only cell type that correlated significantly after multiple testing correction with "overall" mucosal inflammation quantified by the tissue molecular inflammation score (bMIS_UC) (Fig. 4e). Therefore, we hypothesized that Th17 cells, which recruit neutrophils, could be drivers of steroid non-response and would be enriched in colitis tissue of steroid non-responders. To test this, we reanalyzed single-cell transcriptomic data from $CD4^+$ and $CD8^+$ T cells isolated from colon biopsies of 37 patients with ICI colitis from three studies[25–27]. All patients who had been administered second-line immunosuppression were considered steroid non-responders. All studies comprised both steroid responders and non-responders; 70.3% of patients were steroid-naïve upon endoscopy. After correction of study-specific batch effect (Supplementary Fig. 4a, b)[14], unsupervised clustering yielded 48 T cell clusters (Supplementary Fig. 4c), with $CD4^+$ and $CD8^+$ T cell clusters clearly separated (Supplementary Fig. 4d, e). Clusters representing Th17 and Th22 cells were identified based on expression of *IL17A* and *IL22* (Fig. 4f). In contrast to our hypothesis, Th17/Th22 cells, as well as other $CD4^+$ and $CD8^+$ T cell clusters, were equally abundant in tissue of responders and non-responders (Fig. 4g) (Supplementary Fig. 4f). This could be explained by subsets of Th17 cells differing in their pro-inflammatory capacity, with pathogenic Th17.1 cells particularly associated with steroid resistance in autoimmune disease[23]. However, steroid responder and non-responder biopsies were also equally enriched for a published Th17.1 signature[23], both in bulk tissue and within Th17/Th22 cells in $CD4^+$ T cell transcriptomic data (Fig. 4h, i). In fact, $CD4^+$ and $CD8^+$ T cells combined from responders and non-responders were transcriptionally virtually identical, with no single gene differentially expressed at $P_{adj} < 0.05$ (data not shown). Besides true biological similarity, this could also indicate inadequate allocation of patients to one of both steroid response categories, since this allocation was based on published clinical metadata on immunosuppressant use (not steroid response).

Taken together, type 1 and type 17 responses are more pronounced in colitis tissue of non-responders, but we found no evidence supporting that this difference is driven by mechanistical involvement of Th17 cells, in particular pathogenic Th17.1 cells, in steroid-unresponsive ICI colitis.

Discussion

Current irAE treatment strategies relying on empirical use of high-dose steroids in first-line and targeted immunosuppression for steroid-refractory cases are suboptimal, since both high-dose steroids and second-line immunosuppressants for irAEs have been associated with worse survival. However, use of alternative strategies that can limit cumulative immunosuppression exposure, including early use of targeted immunosuppressants, and optimal candidate selection for such approach is limited by insufficient knowledge of irAE pathogenesis, including poor understanding of steroid resistance mechanisms. In the present study, we took a multi-omics approach using blood and tissue from patients with mostly gastro-intestinal irAEs, to identify pre-steroids predictors of response and characterize immunological patterns associated with steroid non-response. In summary, steroid non-response was reflected in blood by trends for increased Tc1-like $CD8^+$ T cells and serum IL-17, IL-6, IL-12 and IL-23 before, and persistent T cell activation and proliferation after initiation of steroids. In colitis tissue, an enhanced mixed type 1/type 17 immune response showed the strongest association with steroid non-responsive versus steroid-responsive colitis. While activated $CD4^+$ memory T cells were enriched in colitis tissue of non-responders, detailed analysis of tissue $CD4^+$ and $CD8^+$ T cells in a larger cohort did not support the involvement of specific T cell subsets in steroid-unresponsive irAEs.

We and others have previously shown that mixed type 1/type 17 responses are dominant in irAEs[9,43–45], with type 17 skewing particularly observed after ipilimumab-containing therapy[9,45]. Consistent with previous reports[45,46], we observed trends for elevated IL-17 (as well as IL-6 and IL-17-inducible MMP-3) in serum of non-responders prior to steroid initiation. Furthermore, a type 17 signature was enriched in transcriptomic data from bulk tissue of ICI colitis patients not responding to steroids. These findings are concordant with small studies on blood of ICI arthritis patients suggesting a role for Th17/Tc17 cells in steroid resistance[45,46]. Increased type 17 skewing could simply reflect broader immune activation in the context of severe irAEs. However, because Th17-pathway-directed treatment strategies have already shown promise in treating irAEs while enhancing anti-tumor responses[43,47,48], we explored cues to support whether these therapies could also abrogate steroid resistance in irAEs. Tissue abundance of *IL17A*- and *IL22*-expressing $CD4^+$ clusters was not associated with steroid response. We may have underestimated the abundance of Th17/Th22 cells focusing on $IL17A^+$ and $IL22^+$ clusters, since expression of secreted proteins including cytokines is only moderately reflected on the transcriptomic level[49]. In addition, the entire pool of Th17/Th22 cells may actually represent subsets with different inflammatory potential. Th17 cells, and Th17.1 cells in particular, have been implicated in steroid resistance in various autoimmune diseases, including IBD, Th17-high asthma and multiple sclerosis[23,50,51]. Th17.1 cells feature a pathogenic phenotype (producing both IFN-γ and IL-17) and are specifically associated with *ABCB1*, or multi-drug resistant type 1 (*MDR1*) expression, which actively expels prednisolone and dexamethasone from the cytoplasm[52,53]. Enrichment analysis in colitis tissue of a Th17.1 signature, comprising *ABCB1*, did not reveal an association with steroid response in our cohort either. Taken together, we were unable to demonstrate a role for Th17 cells as drivers of steroid non-response in irAEs, specifically ICI colitis. Apart from the above, several additional factors could explain the discrepancies between blood and bulk RNA-seq data versus scRNA-seq data. First, other sources of IL-17, such as type 3 innate lymphoid cells, could alternatively be responsible for the type 17 signature enrichment in bulk RNA-seq data and increased serum IL-17 in non-responders, whereas Th17 cells were not found enriched in non-responders in scRNA-seq data. Second, the allocation of individuals into

steroid-response groups was based on publicly available metadata on immunosuppressant use provided in the study metadata. These data may not accurately reflect steroid response as strictly defined in our cohort. Moreover, no minimum dosage of systemic steroids has been considered for patients included from scRNA-seq studies.

Although limited by the observational nature of our data, we show that lymphocyte infiltration was lower in tissue of steroid-responding patients within 24 h after initiation of steroids compared to pre-steroids biopsies. Confounding by severity is unlikely, as patients undergoing endoscopy after initiation of steroids on average had higher grade colitis than patients examined pre-steroids. Molecular analysis of mucosal inflammation across timepoints was underpowered, but showed the same trend of lower inflammation in steroid-responders within 24 h of initiation of steroids. Together, these data suggest very early immunological effects of steroids in steroid-responding patients with ICI colitis. As genomic effects of steroids take more than 24 h to come into effect, lower lymphocyte (but not neutrophil) infiltration could be explained by lymphotoxicity through membrane-bound glucocorticoid receptors or other non-genomic mechanisms[54]. Besides steroid-induced apoptosis, peaking after 72 h and primarily affecting activated T cells based on in vitro studies[55,56], redistribution of lymphocytes could also explain their lower tissue abundance. Importantly, molecular indices of mucosal inflammation have not been assessed sooner than 4 weeks after treatment initiation in IBD trials[22].

We also quantitively assessed lymphocyte and neutrophil infiltration in tissue slides of ICI colitis, but found no association with response to steroids. The extent of histologic and endoscopic inflammation, particularly ulceration, has been associated with need for second-line immunosuppression in ICI colitis[57–61]. Histological inflammation measured by the Robarts Histopathology Index (RHI), but not the pattern of inflammation (acute, chronic-active or microscopic), was associated with biological use in multivariate analysis of ICI colitis[62]. In contrast, chronic histological abnormalities, such as basal plasmacytosis and crypt architectural distortion, independently predict relapse in ulcerative colitis[63,64]. The limited amount of data in ICI colitis may thus indicate that histological indices of chronicity in ICI colitis do not necessarily reflect the necessity for treatment escalation. In support of this, time-to-irAE-onset since ICI initiation was not associated with steroid response rates for most irAEs including colitis[65], although time between symptom onset and treatment initiation could constitute a better proxy for chronicity. Neutrophil infiltration is an important criterion in the RHI, worth up to 15 (of maximum 33) points allocated for lamina propria and epithelial neutrophil infiltration. In our study, neither pre-steroids neutrophil, nor lymphocyte infiltration predicted steroid non-response. This may be due to our quantitative approach, lacking qualitive detail on the extent of inflammation and leukocyte distribution patterns. These findings underscore that in standardizing histological evaluation of ICI colitis[66], qualitative aspects of inflammation may hold more prognostic value than purely quantitative criteria.

We are aware that our study has limitations. Despite the large number of prospectively enrolled patients in this hypothesis-generating study and our attempt to achieve better homogeneity by enhancing for gastrointestinal toxicity, sample size did not allow for subgroup analysis stratified by irAE subtype. Therefore, differences between steroid responders and non-responders may be attributable in part to organ-specificity of immune responses. Also, our findings may not be generalizable to other irAE types, like skin or pulmonal irAEs, or other cancer types, since the vast majority of patients in our cohort had melanoma. Specifically within the group of steroid non-responders, biological differences may potentially be distinguished between steroid-resistant/-refractory versus steroid-dependent patients. Definitions of steroid-resistance versus steroid-dependency are not consistently applied within the field of irAEs[35]. Therefore, their biological differences or implications for clinical outcomes are largely unknown. However, if steroid-resistant irAEs were to feature immunologically more severe disease than steroid-dependent irAEs, the latter could have diminished differences between steroid-responders and non-responders in our study. Moreover, the number of patients with irAEs and complete blood sampling was too limited to consider tumor response in addition to ICI type as covariates and to compose an internal validation cohort. Validation of our findings in larger cohorts is thus warranted. Lastly, due to our focus on T cells, we were unable to explore the effect of other interesting cell types potentially involved in similar detail. Our data suggest that certain cytotoxic NK cell subsets may be associated with steroid non-response, an observation supported by previous reports linking NK cell cytotoxicity to irAE occurrence and severity[67,68].

In conclusion, a trend for expansion of a mixed type 1/type 17 immune response in blood of patients with irAEs who are not responding to steroids was reflected by enrichment of especially type 1 and type 17 signatures in ICI colitis tissue, but could not be consolidated by detailed T-helper subset analysis. We provide preliminary molecular and histological evidence that steroids may sort effects in tissue shortly after treatment initiation in steroid-responding patients with irAEs. Furthermore, our translational data may aid in constructing standardized histological evaluation criteria for ICI colitis and inform the design of studies to investigate new treatment strategies for irAEs.

Data availability

Source data underlying the analyses in main and Supplementary Figs. is available in Supplementary Data 1. Data underlying Figs. 2a and 4f, g, i and Supplementary Figs. 2a and 4 are deposited at Zenodo and can be freely accessed via https://doi.org/10.5281/zenodo.16948925. Additional data on the cohorts are available from the corresponding author upon reasonable request, but restrictions may apply to data sharing, especially outside the European Union, due to national legislation and local regulations.

Code availability

All R code used for analyses is available from https://github.com/mickvaneijs/UNICIT/tree/main/response_steroids_irAEs.

Received: 5 March 2025; Accepted: 25 September 2025;
Published online: 18 November 2025

References

1. Suijkerbuijk, K. P. M., van Eijs, M. J. M., van Wijk, F. & Eggermont, A. M. M. Clinical and translational attributes of immune-related adverse events. *Nat. Cancer* **5**, 557–571 (2024).
2. Haanen, J. et al. Management of toxicities from immunotherapy: ESMO Clinical Practice Guideline for diagnosis, treatment and follow-up. *Ann. Oncol.* **33**, 1217–1238 (2022).
3. Brahmer, J. R. et al. Society for Immunotherapy of Cancer (SITC) clinical practice guideline on immune checkpoint inhibitor-related adverse events. *J. Immunother. Cancer* **9**, e002435 (2021).
4. Schneider, B. J. et al. Management of immune-related adverse events in patients treated with immune checkpoint inhibitor therapy: ASCO guideline update. *J. Clin. Oncol.* **39**, 4073–4126 (2021).
5. Verheijden, R. J. et al. Corticosteroids and other immunosuppressants for immune-related adverse events and checkpoint inhibitor effectiveness in melanoma. *Eur. J. Cancer* **207**, 114172 (2024).
6. Verheijden, R. J. et al. Association of anti-TNF with decreased survival in steroid refractory ipilimumab and anti-PD1-treated patients in the dutch melanoma treatment registry. *Clin. Cancer Res.* **26**, 2268–2274 (2020).
7. van Not, O. J. et al. Association of immune-related adverse event management with survival in patients with advanced melanoma. *JAMA Oncol* **8**, 1794–1801 (2022).
8. Verheijden, R. J. et al. Corticosteroids for immune-related adverse events and checkpoint inhibitor efficacy: analysis of six clinical trials. *J. Clin. Oncol.* **42**, 3713–3724 (2024).
9. van Eijs, M. J. M. et al. Toxicity-specific peripheral blood T and B cell dynamics in anti-PD-1 and combined immune checkpoint inhibition. *Cancer Immunol. Immunother.* **72**, 4049–4064 (2023).

10. den Braanker, H., Bongenaar, M. & Lubberts, E. How to prepare spectral flow cytometry datasets for high dimensional data analysis: a practical workflow. *Front. Immunol.* **12**, 768113 (2021).
11. Emmaneel, A. et al. PeacoQC: peak-based selection of high quality cytometry data. *Cytometry A* **101**, 325–338 (2022).
12. Hahne, F. et al. Per-channel basis normalization methods for flow cytometry data. *Cytometry A* **77**, 121–131 (2010).
13. Van Gassen, S. et al. FlowSOM: using self-organizing maps for visualization and interpretation of cytometry data. *Cytometry A* **87**, 636–645 (2015).
14. Hao, Y. et al. Dictionary learning for integrative, multimodal and scalable single-cell analysis. *Nat. Biotechnol.* **42**, 293–304 (2024).
15. Zappia, L. & Oshlack, A. Clustering trees: a visualization for evaluating clusterings at multiple resolutions. *Gigascience* **7**, giy083 (2018).
16. Osa, A. et al. Clinical implications of monitoring nivolumab immunokinetics in non-small cell lung cancer patients. *JCI Insight* **3**, e59125 (2018).
17. Lutter, L. et al. Human regulatory T cells locally differentiate and are functionally heterogeneous within the inflamed arthritic joint. *Clin. Transl. Immunol.* **11**, e1420 (2022).
18. de Jager, W., Prakken, B. J., Bijlsma, J. W. J., Kuis, W. & Rijkers, G. T. Improved multiplex immunoassay performance in human plasma and synovial fluid following removal of interfering heterophilic antibodies. *J. Immunol. Methods* **300**, 124–135 (2005).
19. Newman, A. M. et al. Robust enumeration of cell subsets from tissue expression profiles. *Nat. Methods* **12**, 453–457 (2015).
20. Tosolini, M. et al. Assessment of tumor-infiltrating TCRVγ9Vδ2 γδ lymphocyte abundance by deconvolution of human cancers microarrays. *Oncoimmunology* **6**, e1284723 (2017).
21. Hänzelmann, S., Castelo, R. & Guinney, J. GSVA: gene set variation analysis for microarray and RNA-seq data. *BMC Bioinform.* **14**, 7 (2013).
22. Argmann, C. et al. Biopsy and blood-based molecular biomarker of inflammation in IBD. *Gut* **72**, 1271–1287 (2023).
23. Ramesh, R. et al. Pro-inflammatory human Th17 cells selectively express P-glycoprotein and are refractory to glucocorticoids. *J. Exp. Med.* **211**, 89–104 (2014).
24. Morgan, D. & Tergaonkar, V. Unraveling B cell trajectories at single cell resolution. *Trends Immunol.* **43**, 210–229 (2022).
25. Thomas, M. F. et al. Single-cell transcriptomic analyses reveal distinct immune cell contributions to epithelial barrier dysfunction in checkpoint inhibitor colitis. *Nat. Med.* **30**, 1349–1362 (2024).
26. Luoma, A. M. et al. Molecular pathways of colon inflammation induced by cancer immunotherapy. *Cell* **182**, 655–671.e22 (2020).
27. Gupta, T. et al. Tracking in situ checkpoint inhibitor-bound target T cells in patients with checkpoint-induced colitis. *Cancer Cell* **42**, 797–814.e15 (2024).
28. Sundell, T. et al. Single-cell RNA sequencing analyses: interference by the genes that encode the B-cell and T-cell receptors. *Brief. Funct. Genom.* **22**, 263–273 (2022).
29. Love, M. I., Huber, W. & Anders, S. Moderated estimation of fold change and dispersion for RNA-seq data with DESeq2. *Genome Biol* **15**, 550 (2014).
30. Baumann, E. et al. HoVer-NeXt: a fast nuclei segmentation and classification pipeline for next generation histopathology. in *Proceedings of Machine Learning Research* (2024).
31. Graham, S. et al. Lizard: a large-scale dataset for colonic nuclear instance segmentation and classification. *arXiv* https://doi.org/10.48550/arxiv.2108.11195 (2021).
32. Bankhead, P. et al. QuPath: open source software for digital pathology image analysis. *Sci. Rep.* **7**, 16878 (2017).
33. Butler, H. et al. The GeoJSON Format RFC 7946. https://datatracker.ietf.org/. https://datatracker.ietf.org/doc/rfc7946/ (2017).
34. Naidoo, J. et al. Society for Immunotherapy of Cancer (SITC) consensus definitions for immune checkpoint inhibitor-associated immune-related adverse events (irAEs) terminology. *J. Immunother. Cancer* **11**, e006398 (2023).
35. Daetwyler, E. et al. Corticosteroid-resistant immune-related adverse events: a systematic review. *J. Immunother. Cancer* **12**, e007409 (2024).
36. Nicolet, B. P. et al. CD29 identifies IFN-γ-producing human CD8 + T cells with an increased cytotoxic potential. *Proc. Natl. Acad. Sci. USA* **117**, 6686–6696 (2020).
37. Koenders, M. I. et al. Tumor necrosis factor-interleukin-17 interplay induces S100A8, interleukin-1β, and matrix metalloproteinases, and drives irreversible cartilage destruction in murine arthritis: rationale for combination treatment during arthritis. *Arthritis Rheum* **63**, 2329–2339 (2011).
38. Yagi, Y., Andoh, A., Inatomi, O., Tsujikawa, T. & Fujiyama, Y. Inflammatory responses induced by interleukin-17 family members in human colonic subepithelial myofibroblasts. *J. Gastroenterol.* **42**, 746–753 (2007).
39. Cortez, D. M. et al. IL-17 stimulates MMP-1 expression in primary human cardiac fibroblasts via p38 MAPK- and ERK1/2-dependent C/EBP-beta, NF-kappaB, and AP-1 activation. *Am. J. Physiol. Heart Circ. Physiol.* **293**, H3356–H3365 (2007).
40. Sproston, N. R. & Ashworth, J. J. Role of C-reactive protein at sites of inflammation and infection. *Front. Immunol.* **9**, 754 (2018).
41. Vuyyuru, S. K., Nardone, O. M. & Jairath, V. Predicting outcome after acute severe ulcerative colitis: a contemporary review and areas for future research. *J. Clin. Med*. **13**, 4509 (2024).
42. Wang, R. et al. Clonally expanded CD38hi cytotoxic CD8 T cells define the T cell infiltrate in checkpoint inhibitor-associated arthritis. *Sci. Immunol*. **8**, eadd1591 (2023).
43. Dimitriou, F. et al. A targetable type III immune response with increase of IL-17A expressing CD4 + T cells is associated with immunotherapy-induced toxicity in melanoma. *Nat. Cancer* **5**, 1390–1408 (2024).
44. Franken, A. et al. Single-cell transcriptomics identifies pathogenic T-helper 17.1 cells and pro-inflammatory monocytes in immune checkpoint inhibitor-related pneumonitis. *J. Immunother. Cancer* **10**, e005323 (2022).
45. Kim, S. T. et al. Distinct molecular and immune hallmarks of inflammatory arthritis induced by immune checkpoint inhibitors for cancer therapy. *Nat. Commun.* **13**, 1970 (2022).
46. Thimmapuram, R. et al. Identification of biomarkers predicting steroid resistance in immune checkpoint inhibitor-induced arthritis. *Arthritis Rheumatol.* **75** (2023).
47. Hailemichael, Y. et al. Interleukin-6 blockade abrogates immunotherapy toxicity and promotes tumor immunity. *Cancer Cell* **40**, 509–523.e6 (2022).
48. Fa'ak, F. et al. Selective immune suppression using interleukin-6 receptor inhibitors for management of immune-related adverse events. *J. Immunother. Cancer* **11**, e006814 (2023).
49. Nicolet, B. P. & Wolkers, M. C. The relationship of mRNA with protein expression in CD8 + T cells associates with gene class and gene characteristics. *PLoS One* **17**, e0276294 (2022).
50. Xie, Y., Abel, P. W., Casale, T. B. & Tu, Y. TH17 cells and corticosteroid insensitivity in severe asthma. *J. Allergy Clin. Immunol.* **149**, 467–479 (2022).
51. Koetzier, S. C. et al. Brain-homing CD4 + T cells display glucocorticoid-resistant features in MS. *Neurol. Neuroimmunol. Neuroinflamm.* **7**, e894 (2020).
52. Banuelos, J., Cao, Y., Shin, S. C. & Lu, N. Z. Immunopathology alters Th17 cell glucocorticoid sensitivity. *Allergy* **72**, 331–341 (2017).
53. Devine, K. et al. The ATP-binding cassette proteins ABCB1 and ABCC1 as modulators of glucocorticoid action. *Nat. Rev. Endocrinol.* **19**, 112–124 (2023).
54. Scheschowitsch, K., Leite, J. A. & Assreuy, J. New insights in glucocorticoid receptor signaling-more than just a ligand-binding receptor. *Front. Endocrinol. (Lausanne)* **8**, 16 (2017).

55. Nieto, M. A., González, A., Gambón, F., Díaz-Espada, F. & López-Rivas, A. Apoptosis in human thymocytes after treatment with glucocorticoids. *Clin. Exp. Immunol.* **88**, 341–344 (1992).
56. Lanza, L. et al. Prednisone increases apoptosis in in vitro activated human peripheral blood T lymphocytes. *Clin. Exp. Immunol.* **103**, 482–490 (1996).
57. Abu-Sbeih, H. et al. Importance of endoscopic and histological evaluation in the management of immune checkpoint inhibitor-induced colitis. *J. Immunother. Cancer* **6**, 95 (2018).
58. Cheung, V. T. F. et al. Immune checkpoint inhibitor-related colitis assessment and prognosis: can IBD scoring point the way? *Br. J. Cancer* **123**, 207–215 (2020).
59. Geukes Foppen, M. H. et al. Immune checkpoint inhibition-related colitis: symptoms, endoscopic features, histology and response to management. *ESMO Open* **3**, e000278 (2018).
60. Mooradian, M. J. et al. Mucosal inflammation predicts response to systemic steroids in immune checkpoint inhibitor colitis. *J. Immunother. Cancer* **8**, e000451 (2020).
61. Wang, Y. et al. Novel endoscopic scoring system for immune mediated colitis: a multicenter retrospective study of 674 patients. *Gastrointest. Endosc.* **100**, 273–282.e4 (2024).
62. Pai, R. K. et al. The significance of histological activity measurements in immune checkpoint inhibitor colitis. *Aliment. Pharmacol. Ther.* **53**, 150–159 (2021).
63. Gupta, A., Yu, A., Peyrin-Biroulet, L. & Ananthakrishnan, A. N. Treat to target: the role of histologic healing in inflammatory bowel diseases: a systematic review and meta-analysis. *Clin. Gastroenterol. Hepatol.* **19**, 1800–1813.e4 (2021).
64. Vespa, E. et al. Histological scores in patients with inflammatory bowel diseases: the state of the art. *J. Clin. Med*. **11**, 939 (2022).
65. Ruf, T. et al. Second-line therapies for steroid-refractory immune-related adverse events in patients treated with immune checkpoint inhibitors. *Eur. J. Cancer* **203**, 114028 (2024).
66. Ma, C. et al. Recommendations for standardizing biopsy acquisition and histological assessment of immune checkpoint inhibitor-associated colitis. *J. Immunother. Cancer* **10**, e004560 (2022).
67. Sung, C. et al. Integrative analysis of risk factors for immune-related adverse events of checkpoint blockade therapy in cancer. *Nat. Cancer* **4**, 844–859 (2023).
68. Kim, G. D. et al. Single-cell RNA sequencing of baseline PBMCs predicts ICI efficacy and irAE severity in patients with NSCLC. *J. Immunother. Cancer* **13**, e011636 (2025).

Acknowledgements

We thank the patients, their families and caregivers and healthy donors for their willingness to participate in this study; clinical staff and UNICIT consortium members for contributing to patient accrual, sample collection and biobanking; and the Multiplex Core Facility of the University Medical Center Utrecht for performing the multiplex immunoassays. Figure 1 and icons used in Figs. 2–4 have been created with www.biorender.com. This investigator-initiated study received funding from Bristol Myers Squibb (grant number CA209-6JY), paid to institution.

Author contributions

Conceptualization: M.J.M.v.E., K.P.M.S., F.W. Methodology: M.J.M.v.E., M.M.v.d.W., H.B.K., N.M.M.D., M.S., S.N., K.P.M.S., F.W. Formal analysis: M.J.M.v.E., M.M.v.d.W., H.B.K., M.S. Performing experiments: M.J.M.v.E., M.M.v.d.W., H.B.K., N.M.M.D. Data Curation: M.J.M.v.E., H.B.K., R.J.V., F.D.M.v.S., B.O. Writing - Original Draft: M.J.M.v.E. Writing - Review & Editing: M.J.M.v.E., M.M.v.d.W., H.B.K., N.M.M.D., M.S., R.J.V., F.D.M.v.S., B.O., S.N., K.P.M.S., F.W. Supervision: K.P.M.S., F.W. Funding acquisition: M.J.M.v.E., K.P.M.S., F.W.

Competing interests

M.J.M.v.E., M.M.v.d.W., H.B.K., N.M.M.D., M.S., R.J.V., F.D.M.v.S., B.O., S.N.: none. K.P.M.S.: Consulting/advisory relationship: Abbvi,e, Sairopa. Research funding: TigaTx, Bristol Myers Squibb, Philips, Genmab, Pierre Fabre. Honoraria: Bristol Myers Squibb. All paid to institution. F.W.: has advisory relationships with Janssen and Takeda, and received research funding from Takeda, Galapagos, BMS, Sanofi, and Leo Pharma.

Additional information

Supplementary information The online version contains supplementary material available at https://doi.org/10.1038/s43856-025-01164-3.

Correspondence and requests for materials should be addressed to Femke van Wijk.

Peer review information *Communications Medicine* thanks the anonymous reviewers for their contribution to the peer review of this work. A peer review file is available.

the UNICIT Consortium

Bas Oldenburg[5], Karijn P. M. Suijkerbuijk[1,6] & Femke van Wijk[2]

A full list of members and their affiliations appears in the Supplementary Information.